ISSN 0208-7774 TRIBOLOGIA 1/2022 p. 65–73
DOI: 10.5604/01.3001.0015.8985

Katarzyna PIOTROWSKA*, Monika MADEJ**

INFLUENCE OF THIN COATINGS FORMED BY ALD TECHNIQUES ON THE PROPERTIES OF Ti13Nb13Zr TITANIUM ALLOY

WPŁYW CIENKICH POWŁOK WYTWARZANYCH TECHNIKĄ ALD NA WŁAŚCIWOŚCI STOPU TYTANU Ti13Nb13Zr

Key words: ALD technique, friction, hardness, surface texture, titanium alloys, wear.

Abstract: The article evaluates the properties of oxide films: Al_2O_3 and TiO_2, deposited using the ALD method on the Ti13Nb13Zr alloy. It presents the results of examining the geometrical structure of the surface, nanohardness and tribological tests. The surface's geometrical structure was tested through optical microscopy, and nanohardness was determined using the instrumental indentation method with a Berkovich indenter. The modelling tribological tests were performed in a reciprocating motion under the conditions of technically dry friction and with lubrication using Ringer's solution. An analysis of the results of tribological tests indicates that the films were characterised by lower motion resistances and wear with respect to the Ti13Nb13Zr alloy. Hardness measurements indicate that, as a result of deposition of the films, the hardness increased by approximately 51% in the case of the Al_2O_3 film and by approximately 44% in the case of the TiO_2 coating. The produced test results constitute a source of knowledge about the Ti13Nb13Zr alloy, oxide films and the possibilities of their potential application to low-load biotribological systems.

Słowa kluczowe: technika osadzania ALD, stopy tytanu, struktura geometryczna powierzchni, tarcie, twardość, zużycie.

Streszczenie: W artykule dokonano oceny właściwości warstw tlenkowych: Al_2O_3 i TiO_2 osadzonych metodą ALD na stopie Ti13Nb13Zr. Przedstawiono wyniki badań struktury geometrycznej powierzchni, nanotwardości oraz testów tribologicznych. Strukturę geometryczną powierzchni zbadano przy użyciu mikroskopii optycznej, a nanotwardość określono metodą instrumentalnej indentacji przy użyciu wgłębnika Berkovich'a. Modelowe badania tribologiczne przeprowadzono w ruchu posuwisto-zwrotnym w warunkach tarcia technicznie suchego oraz ze smarowaniem płynem Ringera. Analiza wyników badań tribologicznych wskazała, że powłoki charakteryzowały się mniejszymi oporami ruchu oraz zużyciem w odniesieniu do stopu Ti13Nb13Zr. Pomiary twardości wskazują, że w wyniku osadzenia powłok twardość wzrosła o około 51% w przypadku powłoki Al_2O_3 oraz o około 44% w przypadku powłoki TiO_2. Uzyskane wyniki badań stanowią źródło wiedzy na temat stopu Ti13Nb13Zr, powłok tlenkowych oraz możliwości ich potencjalnego zastosowania w niskoobciążonych systemach biotribologicznych.

INTRODUCTION

For the last several decades, there has been a considerable amount of technological progress in terms of the production of engineering biomaterials of high importance for medicine. The problem of tribocorrosive wear is a commonly known phenomenon, particularly dangerous in the case of biomedical materials. When entering body fluids, the products of wear can cause inflammation, allergies and, as a result, lead to the rejection of an implant. Tribological and corrosive wear usually affects implants and prostheses.

The most frequently used biomaterials include metallic materials, among which titanium alloys are the most popular. This results from the unique

* ORCID: 0000-0001-6366-2755. Kielce University of Technology, Faculty of Mechatronics and Mechanical Engineering, Tysiąclecia Państwa Polskiego 7 Ave., 25-314 Kielce, Poland.
** ORCID: 0000-0001-9892-9181. Kielce University of Technology, Faculty of Mechatronics and Mechanical Engineering, Tysiąclecia Państwa Polskiego 7 Ave., 25-314 Kielce, Poland.

properties of these materials: high biocompatibility and fatigue strength, an elastic modulus similar to the modulus of human bone, and high resistance to solution in the environment of tissues and body fluids **[L. 1–4]**. Despite having very good physicochemical properties, titanium alloys are characterised by low resistance to friction wear. Due to the above, the paper's authors suggested modifying their top layer by using surface engineering methods.

The use of modern film deposition techniques allows for generating surfaces with improved mechanical and tribological properties, which directly translates into extending the lifetime of a tribological system **[L. 5**, **6]**.

Modifying the top layer through the deposition of surface films influences the improvement of mechanical, tribological, corrosive and fatigue properties of the biomaterials used to date. There are numerous methods for constituting the top layer, among which the Atomic Layer Deposition (ALD) method is one of the most prospective techniques for applying layers several nanometres in thickness. The ALD technique allows depositing a wide range of films: oxides – Al_2O_3, TiO_2, ZrO_2, ZnO, metals – Cu, Co, Fe, Ni and Ag, and other hydroxyapatite **[L. 7–9]**. It is a type of technique for chemical deposition from the gas phase (CVD), which in the process usually uses two precursor gases, which are transported to the reaction zone in an alternating sequence of precisely controlled pulses. The excess amount of unreacted precursors in the deposition chamber is purged with an inert gas – usually nitrogen. This purging results in a self-limiting nature of the surface chemical reactions on the substrate, and in this way, no more than a single layer of the precursor remains on the surface after purging. In ideal cases, ALD may provide perfect control of thickness at a level of 1 Å and create a uniform film on elements with a complicated geometry **[L. 10–13]**. The method is characterised by complete control of the process, in terms of both the pressure and the temperature, the possibility to deposit layers in low temperatures, the repeatability of the process and high efficiency **[L. 10, 13–15]**.

The present paper aims to evaluate the properties of oxide films: Al_2O_3 and TiO_2, deposited using the ALD technique on the Ti13Nb13Zr titanium alloy.

MATERIALS AND METHODS

The Al_2O_3 and TiO_2 oxide films were deposited using the ALD technique on the Ti13Nb13Zr titanium alloy using the Beneq system. The chemical composition of the alloy and its basic mechanical properties are presented in **Tables 1** and **2.**

Table 1. Chemical composition of Ti13Nb13Zr titanium alloy, % wag
Tabela 1. Skład chemiczny stopu tytanu Ti13Nb13Zr w % wag

Element	% weight							
	C	**H**	**O**	**N**	**Fe**	**Nb**	**Zr**	**Ti**
Ti13Nb13Zr	≤ 0.08	≤ 0.015	≤ 0.016	≤ 0.05	≤ 0.25	12.5-14.0	12.5-14.0	based

Table 2. Mechanical properties of the Ti13Nb13Zr alloy
Tabela 2. Właściwości mechaniczne stopu Ti13Nb13Zr

Material	Rm [MPa]	Re [MPa]	A [%]	Z [%]	E [GPa]
Ti13Nb13Zr	973-1037	836-908	10-16	27-53	79-84

The key step of preparing samples for the tests involves grinding and polishing their surfaces. Proper selection of the processing parameters influences the functional properties of the machined elements. Samples in the shape of discs, 30 mm in diameter and 5 mm in height, were ground using a grinder-polisher from the Pace Technologies company. The sandpapers were made of silicon carbide, with the grain size increased from 120 to 4000 µm. The finishing consisted of polishing on cloth with ad addition of diamond paste with a grain size of 1 µm. After the grinding and polishing process, the resulting surface roughness values of the samples were approximately Ra = 60 nm. The remaining amplitude parameters of the reference surface are presented in **Table 4**. Prior to deposition of the films, the samples were defatted in ethyl alcohol in an ultrasonic cleaner.

The process of depositing films using the chemical deposition method of thin atomic layers from the gas phase – ALD – used three precursors ($TiCl_4$, TMA and H_2O). Titanium Tetrachloride ($TiCl_4$) and water (H_2O) were used to produce the TiO_2 film. On the other hand, the Al_2O_3 film consisted of Trimethylaluminium (TMA) and H_2O. In order to create the film, 1000 cycles were used, and the process was performed at a temperature of 150°C. After the deposition process using a reflectometer, the thickness of the deposited films was measured, ranging from 150 to 170 nm.

A Leica DCM8 confocal microscope was used to measure the geometrical structure of the surface before and after the tribological tests. The results of these tests included axonometric images of the studied surfaces and selected generated amplitude parameters for the profiles forming the surface.

The tribological tests were performed using an NTR[3] nano tribometer from the Anton Paar company. The tests were conducted in a reciprocating motion, under the conditions of technically dry friction and friction with lubrication using Ringer's solution – an agent simulating a body fluid. The chemical composition of the lubricant is presented in **Table 3**.

Table 3. Chemical composition of the lubricant – Ringer's solution
Tabela 3. Skład chemiczny środka smarowego – płynu Ringera

Skład chemiczny [g/dm^3]		
NaCl	KCl	$CaCl_2$
8.6	0.3	0.243

The tribological tests used a load force of 5 mN and a frequency of 1 Hz. In the tested friction pairs, a sphere with a diameter of 2 mm made of aluminium oxide (III) served as a counter-specimen. The layout of a friction pair is presented in **Fig. 1**. The tribological tests were repeated three times for each sliding pair with the given parameters. The geometrical structures of frictionally engaging surfaces were examined after the tribological tests.

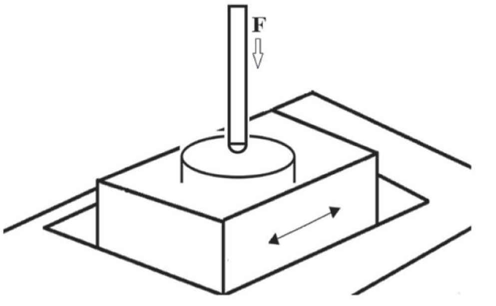

Fig. 1. Friction pair
Rys. 1. Schemat węzła tarcia

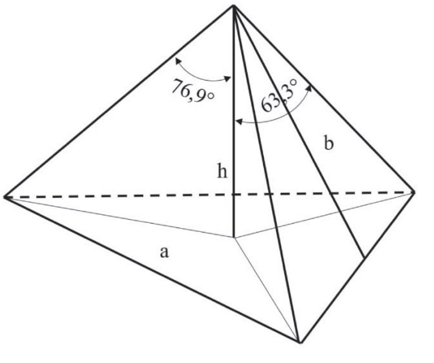

Fig. 2. Geometry of Berkovich indenter
Rys. 2. Geometria wgłębnika Berkovicha

The instrumental indentation method is used to determine the most important mechanical parameters: the hardness and the elasticity of the films. The hardness of the Ti13Nb13Zr alloy and the films – TiO_2 and Al_2O_3 – was determined using an Anton Paar Ultra Nano Hardness Tester (UNHT). The tests used an indenter with a Berkovich geometry and a rounding radius of 100 nm. The adopted constant loading and unloading rate was 0.1 mN/min, with a maximum load of 0.05 mN and a pause of 1 s. The geometry of the indenter is presented in **Figure 2**.

RESULTS

The results of the tests include presentation of the surface in the form of an axonometric image, and compilations of profiles making up this surface, both for reference samples and for films. The respective average profiles were generated for each one of the samples based on 100 profiles. The amplitude parameters (according to ISO 4287) are presented in **Table 4.**

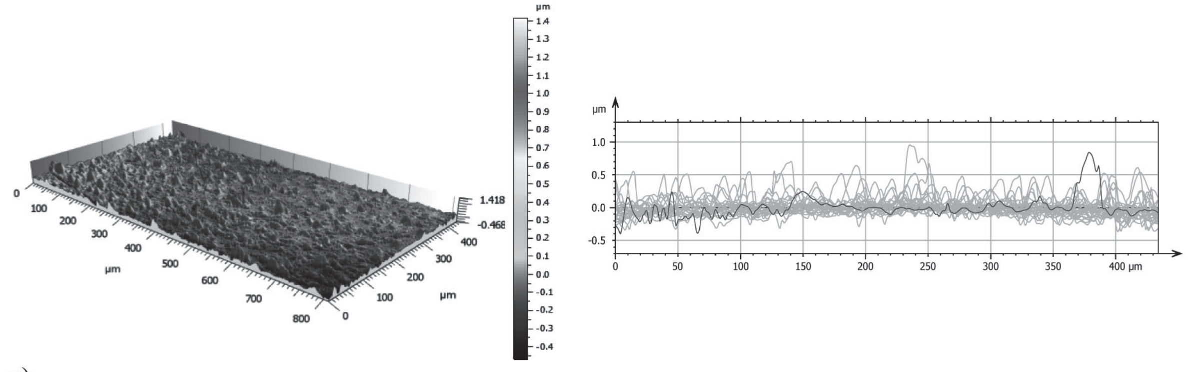

a)

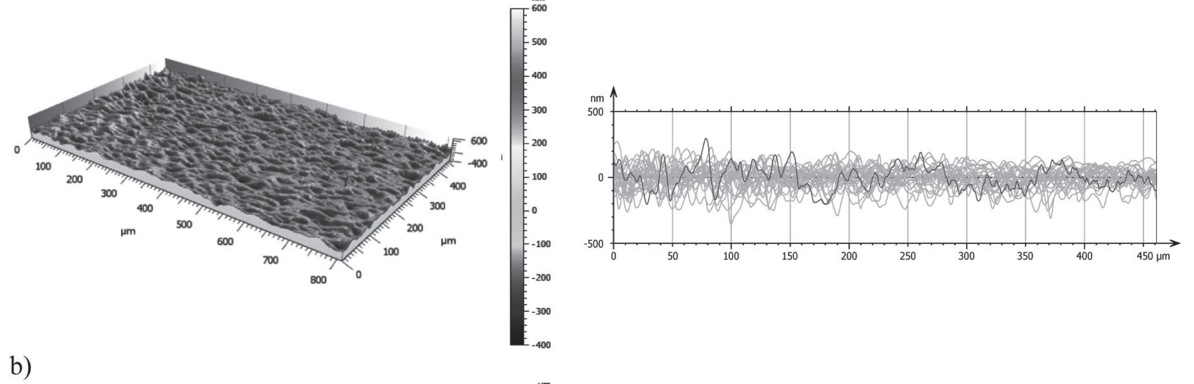

b)

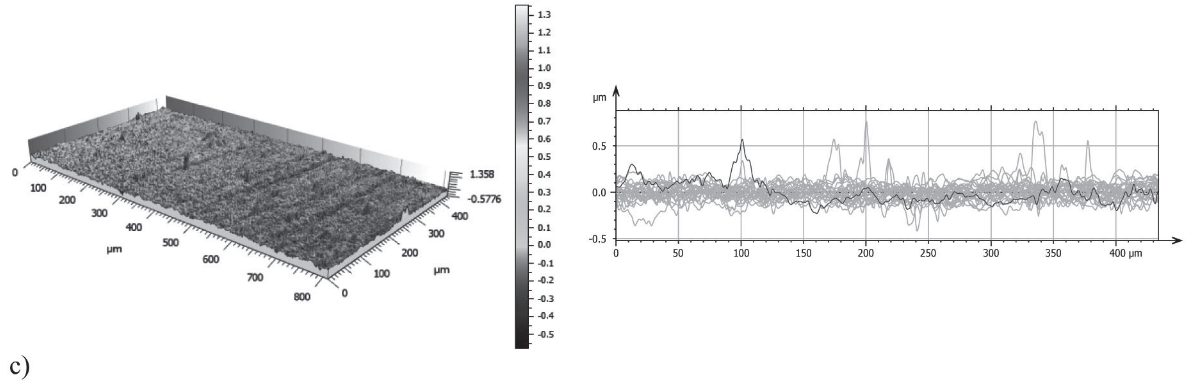

c)

Fig. 3. The i axonometric image of surface texture a) Ti13Nb13Zr, b) Ti13Nb13Zr Al_2O_3, c) Ti13Nb13Zr TiO_2

Rys. 3. Obrazy aksonometryczne struktury geometrycznej powierzchni a) Ti13Nb13Zr, b) Ti13Nb13Zr Al_2O_3, c) Ti13Nb13Zr TiO_2

Table 4. The parameters of surface texture

Tabela 4. Parametry amplitudowe

Parameter	Ti13Nb13Zr reference		Ti13Nb13Zr Al_2O_3		Ti13Nb13Zr TiO_2	
	mean	stand. dev.	mean	stand. dev.	mean	stand. dev.
Rp [nm]	390	90	173	44	200	40
Rv [nm]	170	50	188	52	150	60
Ra [nm]	60	20	58	13	40	10
Rq [nm]	90	30	74	16	60	10
Rsk	1.5	0.75	-0.23	0.39	0.32	0.26
Rku	6.77	1.62	3.04	0.64	3.54	0.49

An analysis of the amplitude parameters proved that the most developed surface topography characterised the reference sample. This is indicated by the values of the characteristic parameters: *Rp, Rv, Ra, Rq, Rsk and Rku*. A positive value of the *Rsk* parameter indicates the presence of steep elevations with acute vertices on the surface of this sample. A drop in the value of this parameter down to 0.32 in the case of Ti13Nb13Zr TiO_2 indicates gradual flattening of this surface. A negative *Rsk* value of the Ti13Nb13Zr Al_2O_3 sample proves the plateau-like shape of its surface – gentle slopes and rounded vertices. The coefficient of concentration, commonly called *kurtosis* (*Rku*) – constituted a measure of the slenderness of the ordinate distribution curve. Similarly to *Rsk*, it is sensitive to individual elevations or indentations. A value close to 3 indicates a normal distribution of ordinates, which is true in the case of the films (TiO_2, Al_2O_3). The kurtosis of the reference sample is twice as high compared to the values produced for the films; it proves that the sample made of the Ti13Nb13Zr titanium alloy had the most developed surface.

The geometrical structure of the engaging surfaces directly impacts the intensity of the wear process and the value of the coefficient of friction. A detailed analysis of surface topography enables preliminary prediction of the tribological properties of material already at the stage of constituting its top layers.

Figure 4 presents the results of testing the instrumental hardness, Young's modulus and the maximum value of indentation h_{max}. The results presented on the graphs are averages determined based on ten measurements.

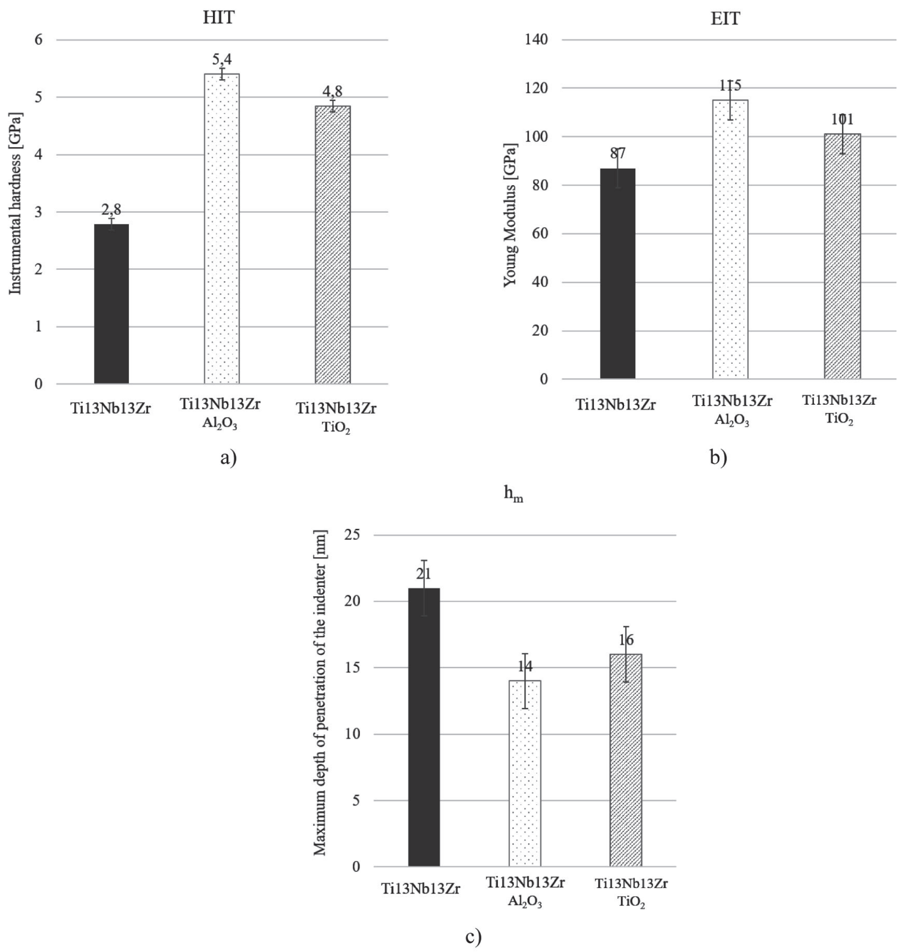

Fig. 4. Results of mechanical tests a) instrumental hardness (HIT), Young's modulus (EIT), the penetration depth of the indenter (hm)

Rys. 4. Wyniki badań mechanicznych a) twardość instrumentalna (HIT), moduł Younga (EIT), głębokość penetracji wgłębnika (hm)

The results of mechanical tests have shown that the deposition of oxide films on Ti13Nb13Zr increased the hardness of the alloy, with the highest efficiency (approximately 50%) obtained for the Al_2O_3 film. In the case of TiO_2, the discussed parameter increased by approximately 40%. The penetration depth of the indenter is strictly associated with instrumental hardness. In the case of the reference sample, at the time of reaching the maximum loading force of 0.05 mN, the Berkovich indenter was at a depth of 21 nm. Based on the produced results, it was also concluded that the use of anti-wear layers influenced a slight increase in Young's modulus.

Figure 5 presents the results of the average friction coefficients μ recorded during the cooperation of the tested friction pairs

The performed tests indicate that the TiO_2 film was characterised by the lowest coefficient of friction, both during technically dry friction and during friction with lubrication using Ringer's solution. Moreover, it was noticed that using a lubricant influenced the reduction of motion resistances in all the tested friction pairs. In the case of the reference sample and the Al_2O_3 film, the coefficient of friction decreased by approximately 40%; in the case of the TiO_2 film, the coefficient was lower by half compared to friction without lubrication.

The mutual engagement of elements rubbing against each other results in tribological wear, which is largely dependent on the stereometric properties of the surfaces of triboelements. This applies to both the tests performed under the

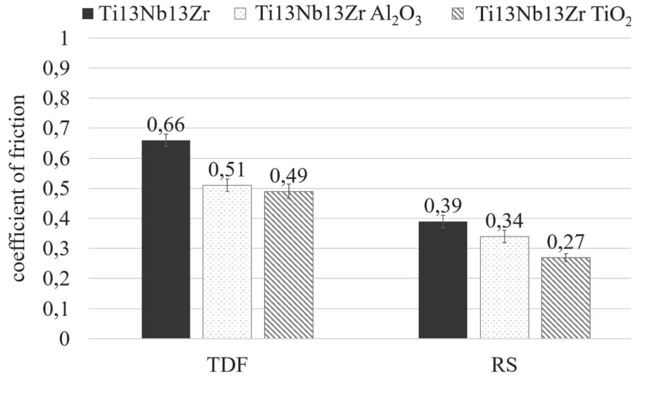

Fig. 5 Mean coefficient of friction during technical dry friction (TDF) and Ringer solution (RR)
Rys. 5. Średnie współczynniki tarcia podczas: tarcia technicznie suchego (TDF), tarcia ze smarowaniem płynem Ringera (RR)

conditions of dry friction as well as with lubrication. The mean wear depth (MWD) and the mean worn surface area (MAA) were determined based on five measurement series. The standard deviation is indicated as σ. The test results are presented in **Figures 6–7**.

An analysis of the microscopic tests of samples upon technically dry friction indicated that the Al_2O_3 film was characterised by the lowest wear in a friction pair with the sphere. The recorded wear was lower by approximately 45% compared to the TiO_2 film and lower by 60% relative to the reference sample. The largest worn surface area was observed on the sample made of Ti13Nb13Zr, which was characterised by the highest development of the surface geometrical structure. The observations of the traces of wear also allowed for determining the wear mechanism. In the case of technically dry friction, there was a prevalence of abrasive and adhesive wear. This is proven by the presence of an uplift of the peripheries of the wear edges (the so-called burr).

A comparative analysis of the generated wear profiles obtained in a cross-section of samples after technically dry friction and after friction in the environment of Ringer's solution indicates that, in the case of the reference sample and the Al_2O_3 film, the use of a lubricant caused the wear to increase by approximately 35%. The tests performed for the TiO_2 film indicated that the layer is characterised by higher resistance to friction wear under lubrication conditions. The measured indentation was four times smaller compared to the value recorded during technically dry friction. The performed tests also indicated that numerous loose wear products were observed in all cases. These particles had an impact on the intensification of the wear processes.

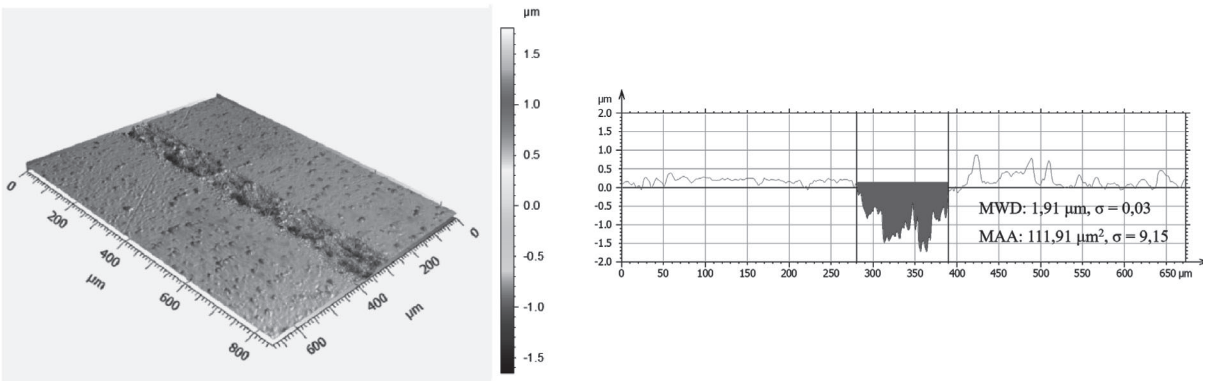

a)

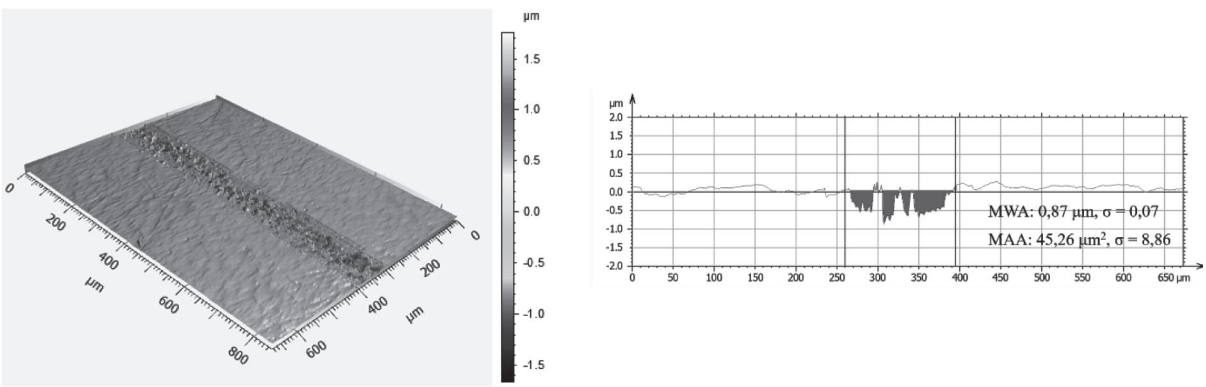

b)

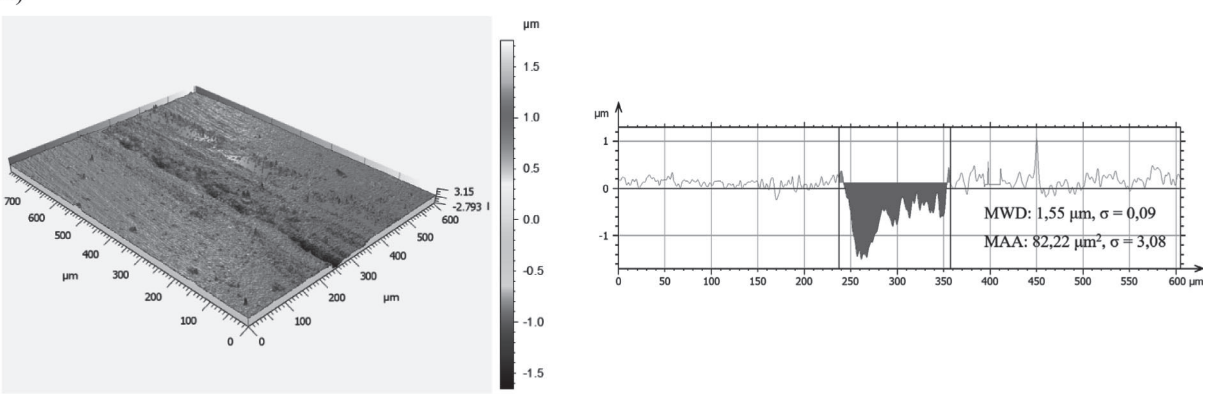

c)

Fig. 6. The axonometric image of the trace of wear and the wear profile in a cross-section for technically dry friction: a) Ti13Nb13Zr, b) Ti13Nb13Zr Al_2O_3, c) Ti13Nb13Zr TiO_2

Rys. 6. Obrazy aksonometryczne śladów wytarcia na przekroju poprzecznym podczas tarcia technicznie suchego a) Ti13Nb13Zr, b) Ti13Nb13Zr Al_2O_3, c) Ti13Nb13Zr TiO_2

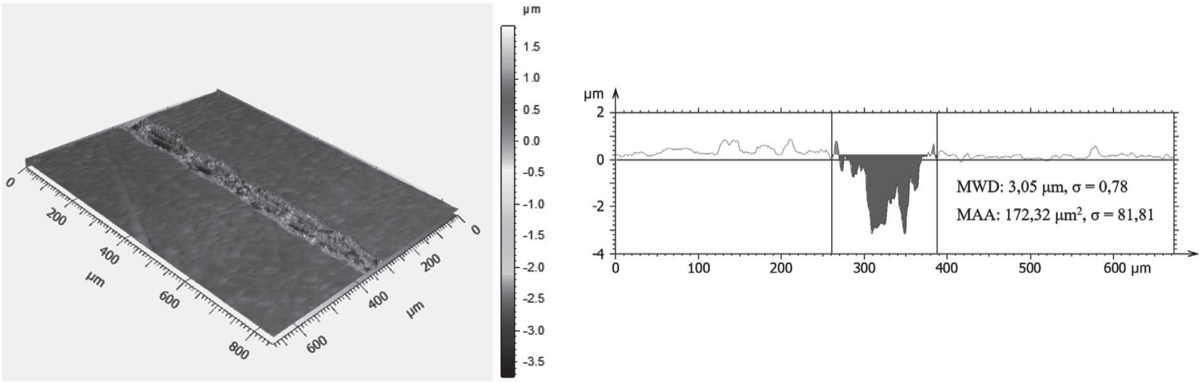

a)

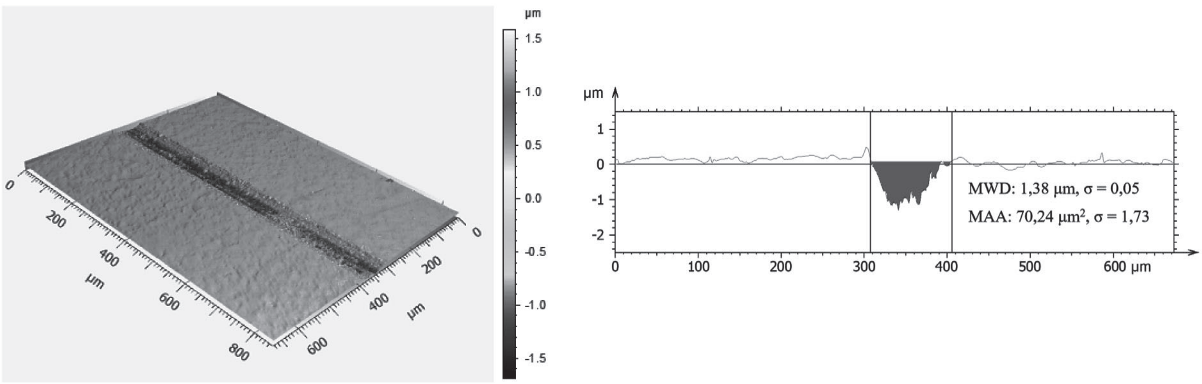

b)

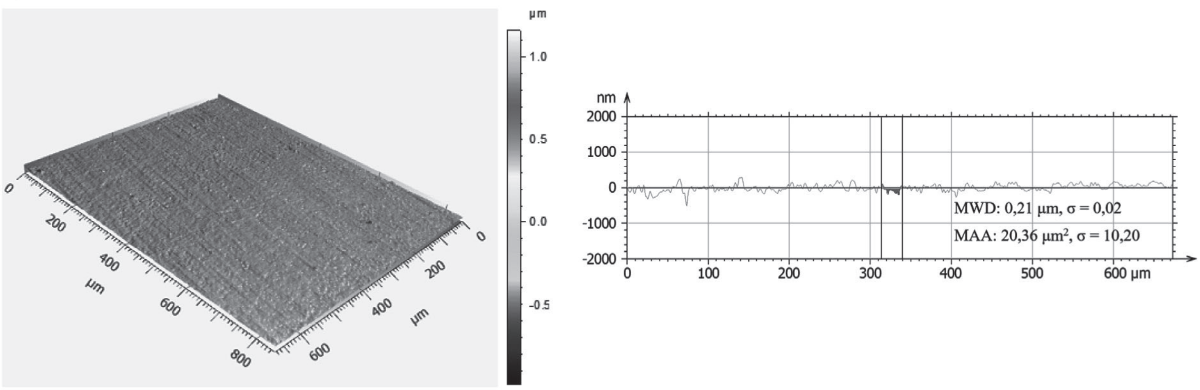

c)

Fig. 7. The axonometric image of the trace of wear and the wear profile in a cross-section during friction in a Ringer's solution environment a) Ti13Nb13Zr, b) Ti13Nb13Zr Al_2O_3, c) Ti13Nb13Zr TiO_2

Rys. 7. Obrazy aksonometryczne śladów wytarcia na przekroju poprzecznym podczas tarcia w środowisku roztworu Ringera: a) Ti13Nb13Zr, b) Ti13Nb13Zr Al_2O_3, c) Ti13Nb13Zr TiO_2

CONCLUSIONS

The performed tribological tests and observations of wear traces confirmed the previous assumption that the heaviest tribological wear characterises the reference sample. The highest friction and wear coefficients were noticed for samples with the most developed surface topography, i.e., the reference sample – the Ti13Nb13Zr alloy. Moreover, it was noticed that the use of Ringer's solution influenced the reduction of motion resistances in all the tested friction pairs: in the case of the reference sample and the Al_2O_3 film – by approximately 40%; in the case of the TiO_2 film – by approximately 50% compared to friction without lubrication.

The application of advanced optical microscopy also allowed for a preliminary evaluation of the wear mechanisms. Based on the axonometric images after tribological tests, it was concluded that abrasive and adhesive wear was predominant in all the studied cases. This is evidenced by furrows, most likely generated due to the displacement of loose products of wear in the work area and the uplift of the peripheries of the edges of wear traces.

The results of mechanical tests proved that the deposition of oxide films resulted in an increase in the hardness of the Ti13Nb13Zr titanium alloy. In the case of using the Al_2O_3 film, the hardness of the alloy increased by approximately 50%; in the case of TiO_2 – by approximately 40%. Based on the produced results, it was also concluded that the use of anti-wear layers influenced a slight increase in Young's modulus. The performed tests unambiguously indicate that the TiO_2 film is the most efficient one in terms of its mechanical and tribological properties.

REFERENCES

1. Dąbrowski R.: The microstructure and properties of Ti13Nb13Zr alloy for biomedical applications, Mechanika w medycynie, 2014, pp. 52–62.
2. Piotrowska K., Granek A., Madej M.: Assessment of Mechanical and Tribological Properties of Diamond-Like Carbon Coatings on the Ti13Nb13Zr Alloy, Open Engineering 2020, 10, pp. 536–545.
3. Gałuszka G., Madej M., Ozimina D., Kasińska J., Gałuszka R.: The characterisation of pure titanium for biomedical applications, Metalurgija 2017, 56 (1–2), pp. 191–194.
4. Basiaga M., Walke W., Kajzer A., Kajzer W., Staszuk M., Kurtyka P.: Adhesion of SiO_2 deposited by means of SOL-GEL and ALD methods on 316LVM steel, Engineering of biomaterials 2017, 141, pp. 13–19.
5. Sęp J., Gałda L., Pawlus P., Koszela W.: Wybrane technologiczne metody zwiększania odporności na zużycie tribologiczne, Tribologia 2008, 4, pp. 59–68.
6. Kalbarczyk M., Michalczewski R., Piekoszewski W., Szczerek M.: Tribological and nano-scale research on model friction couples intended for hip joint prostheses, Tribology – Materials Surfaces & Interfaces 2009, 3(4), pp. 189–195.
7. Dias V.M., Chiappim W., Fraga M.A., Maciel H.S., Marciano F.R., Pessoa R.S.: Atomic Layer Deposition of TiO_2 and Al_2O_3 Thin Films for the Electrochemical Study of Corrosion Protection in Aluminum Alloy Cans Used in Beverage, Materials Research Express 2020, 7, pp. 1–13.
8. Im H., Wittenberg N.J., Lindquist N.C., Oh S.H.: Atomic Layer Deposition (ALD): A Versatile Technique for Plasmonics and Nanobiotechnology, J Mater Res 2012, 27, pp. 663–671.
9. Basiaga M., Walke W., Nakonieczny D., Hyla A.: Physiochemical properties of TiO_2 nanoparticle thin films deposited on stainless steel, Metalurgija 2017, 56 (1–2), pp. 171–174.
10. Johnson R. W., Hultqvist A., Bent S. F.: A Brief Review of Atomic Layer Deposition: From Fundamentals to Applications, Materials Today 2014, 17, pp. 236–246.
11. Boryło P., Łukaszewicz K., Szindler M., Kubacki J., Balin K., Basiaga M., Szewczenko J.: Structure and properties of Al_2O_3 thin films deposited by ALD process, Vacuum 2016, 131, pp. 319–326.
12. Piotrowska K., Madej M., Influence of TiO_2 coating deposited with the ALD technique on the properties of Ti13Nb13Zr titanium alloy, Metalurgija 2022, 61 (3–4), pp. 665–668.
13. Radi P.A., Testoni G. E., Pessoa R. S., Maciel H. S., Rocha L. A., Vieira L., Tribocorrosion behavior of TiO_2/Al_2O_3 nanolaminate, Al_2O_3, and TiO_2 thin films produced by atomic layer deposition, Surface & Coatings Technology 2018, 349, pp. 1077–1082.
14. Bilo F., Borgese L., Prost J., Rauwolf M., Turyanskaya A., Wobrauschek P., Kregsamer P., Streli C., Pazzaglia U., Depero L.E.: Atomic layer deposition to prevent metal transfer from implants: an X-Ray Fluorescence study, Applied Surface Science 2015, vol. 202, pp. 36–42.
15. Zhong Q., Yan J., Qian X., Zhang T., Zhang Z., Li A.: Atomic layer deposition enhanced grafting of phosphorylcholine on stainless steel for intravascular stents, Colloids and Surfaces B: Biointerfaces 2014, vol. 121, pp. 238–247.